

# Gankyrin-mediated interaction between cancer cells and tumor-associated macrophages facilitates prostate cancer progression and androgen deprivation therapy resistance

Guang Peng<sup>a,b,c,\*</sup>, Chao Wang<sup>a,d,\*#</sup>, Hongru Wang<sup>e\*</sup>, Min Qu<sup>f\*</sup>, Keqin Dong<sup>g\*</sup>, Yongwei Yu<sup>h</sup>, Yuquan Jiang<sup>b,i</sup>, Sishun Gan<sup>e</sup>, and Xu Gao<sup>f</sup>

<sup>a</sup>Department of Urinary Surgery, Gongli Hospital of Shanghai Pudong New Area, Shanghai, China; <sup>b</sup>Department of Orthopedic, Joint Logistic Support Force No. 925 Hospital of PLA, Guiyang, China; <sup>c</sup>Department of Burns and Plastic Surgery, General Hospital of Southern Theater Command of PLA, Guangzhou, China; <sup>d</sup>Shanghai Health Commission Key Lab of Artificial Intelligence (AI)-Based Management of Inflammation and Chronic Diseases, Gongli Hospital of Shanghai Pudong New Area, Shanghai, China; <sup>e</sup>Department of Urinary Surgery, The Third Affiliated Hospital of Second Military Medical University (Eastern Hepatobiliary Surgery Hospital), Shanghai, China; <sup>f</sup>Department of Urology, Changhai Hospital, Second Military Medical University, Shanghai, China; <sup>g</sup>Department of Urology, Chinese PLA general hospital of central theater command, Wuhan, China; <sup>h</sup>Department of Pathology, Changhai Hospital, Second Military Medical University, Shanghai, China; <sup>i</sup>Central Lab of Joint Logistic Support Force No. 925 Hospital of PLA, Guiyang, China

## ABSTRACT

Increasing evidence reveals that the interaction between tumor cells and tumor-associated macrophages (TAMs) facilitates the progression of prostate cancer, but the related mechanisms remained unclear. This study determined how gankyrin, a component of the 19S regulatory complex of the 26S proteasome, regulates the progression and androgen deprivation therapy (ADT) resistance of prostate cancer through tumor cell–TAM interactions. *In vitro* functional experiments and *in vivo* subcutaneous tumor models were used to explore the biological role and molecular mechanisms of gankyrin in prostate cancer cell–TAM interactions. 234 prostate cancer patients were randomly divided into training and validation cohorts to examine the prognostic value of gankyrin through immunohistochemistry (IHC) and statistical analyses, and high gankyrin expression was correlated with poor prognosis. In addition, gankyrin facilitated the progression and ADT resistance of prostate cancer. Mechanistically, gankyrin recruited and upregulated non-POU-domain-containing octamer-binding protein (NNO) expression, resulting in increased androgen receptor (AR) expression. AR then bound to the high-mobility group box 1 (HMGB1) promoter to trigger HMGB1 transcription, expression, and secretion. Moreover, HMGB1 was found to promote the recruitment and activation of TAMs, which secrete IL-6 to reciprocally promote prostate cancer progression, ADT resistance and gankyrin expression via STAT3, resulting in formation of a gankyrin/NNO/AR/HMGB1/IL-6/STAT3 positive feedback loop. Furthermore, targeting the interaction between tumor cells and TAMs by blocking this loop inhibited ADT resistance in a tumor xenograft model. Taken together, the data show that gankyrin serves as a reliable prognostic indicator and therapeutic target for prostate cancer patients.

## ARTICLE HISTORY

Received 26 October 2022  
Revised 3 January 2023  
Accepted 23 January 2023

## KEYWORDS



Tumor-associated macrophages; gankyrin; prostate cancer; androgen deprivation therapy; tumor progression

## Introduction

Acquired resistance has been a challenge for prostate cancer treatment since the discovery of the therapeutic effect of androgen receptor (AR) blockade on prostate cancer.<sup>1</sup> Although androgen deprivation therapy (ADT) is initially effective at slowing tumor growth and decreasing prostate-specific antigen (PSA) levels, prostate cancer inevitably becomes hormone insensitive, which is termed castration-resistant prostate cancer (CRPC), after a certain duration of treatment. Recent trials of the second-generation antiandrogen agent enzalutamide, which effectively blocks AR ligand binding, have shown


significantly prolonged progression-free survival and overall survival in CRPC patients with chemotherapy failure.<sup>2,3</sup> However, enzalutamide only offers temporary respite to prostate cancer patients, as therapy resistance often occurs.<sup>4</sup> Therefore, further research is urgently needed to reveal the mechanisms underlying ADT resistance.

During the evolution of prostate cancer from a hormone-sensitive to castration- or treatment-resistant phenotype, persistent activation of AR signaling has been demonstrated to be the key driving force in the development of ADT resistance, occurring through AR splice variants (ARVs), functional

**CONTACT** Chao Wang (Main corresponding author)  [superwang2012@aliyun.com](mailto:superwang2012@aliyun.com)  Department of Urinary Surgery, Gongli Hospital of Shanghai Pudong New Area, 219 Miaopu Road, Shanghai, 200135, China; Gao Xu  [gaoxu.changhai@foxmail.com](mailto:gaoxu.changhai@foxmail.com)  Department of Urology, Changhai Hospital, Second Military Medical University, Shanghai, China; Sishun Gan  [gansishun20101111@163.com](mailto:gansishun20101111@163.com)  Department of Urinary Surgery, The Third Affiliated Hospital of Naval Medical University (Eastern Hepatobiliary Surgery Hospital), 700 North Moyu Road, Shanghai 201805, China; Yuquan Jiang  [jiangyq057@163.com](mailto:jiangyq057@163.com)  Department of Orthopedic Central Lab of Joint Logistic Support Force No. 925 Hospital of PLA, Guiyang, China

\*These authors contributed equally to the study

#Main corresponding author

 Supplemental data for this article can be accessed online at <https://doi.org/10.1080/2162402X.2023.2173422>

© 2023 The Author(s). Published with license by Taylor & Francis Group, LLC.

This is an Open Access article distributed under the terms of the Creative Commons Attribution-NonCommercial License (<http://creativecommons.org/licenses/by-nc/4.0/>), which permits unrestricted non-commercial use, distribution, and reproduction in any medium, provided the original work is properly cited.

mutations or bypass signaling related to glucocorticoid receptors or other kinases.<sup>5,6</sup> Despite lacking the AR ligand-binding domain (LBD), AR-V7, the most well-documented AR splice variant, is a constitutively active variant associated with enzalutamide and abiraterone resistance.<sup>7</sup> Moreover, many studies, including ours, have suggested that prostate carcinoma cells invoke other mechanisms of progression and adaptation to treatments, such as ADT-induced tumor heterogeneity and neuroendocrine differentiation (NED).<sup>8–10</sup>

In fact, extrinsic mechanisms of resistance are driven by the tumor microenvironment (TME), including immune cells and the vasculature.<sup>11,12</sup> Many studies, including ours, have demonstrated that among the immune cells infiltrating the TME, tumor-associated macrophages (TAMs) are highly significant due to their comparatively high abundance and heterogeneous roles in facilitating tumor progression and drug resistance.<sup>13</sup> Moreover, recruitment and retention of disseminated TAMs is driven by tumor cells via various kinds of inflammatory factors, cytokines and pathogens, shifting TAM polarization from antitumorogenic M1 macrophages to the protumorogenic M2 phenotype.<sup>14</sup> Although the results of our study and others have suggested that blocking the regulatory network between tumor cells and TAMs<sup>9,15</sup> might inhibit prostate cancer progression and ADT resistance, the specific mechanisms need to be further studied.

Gankyrin (also known as p28<sup>GANK</sup>, p28 or PSMD10), a component of the 19S regulatory cap of the 26S proteasome, has been identified by our and other previous studies as an oncogene that contributes to oncogenesis, proliferation, drug resistance, and metastasis in multiple types of malignancies.<sup>16–18</sup> In addition, high expression of gankyrin predicts poor prognosis in liver cancer patients.<sup>19</sup> We have also shown that gankyrin can be a prognostic indicator for renal cell carcinoma (RCC) patients and that gankyrin facilitates RCC progression and pazopanib resistance.<sup>20,21</sup> Overall, gankyrin has a critical oncogenic function in the TME, promoting tumor progression and therapy resistance.<sup>22</sup> However, data on its role in prostate cancer are limited. One relevant observation is that higher gankyrin expression has been detected in prostate cancer tissues than in adjacent normal tissues, which correlates positively with a high Gleason score and histopathological tumor grade.<sup>23</sup> Another study reported that downregulation of gankyrin impaired the growth of the prostate cancer cell line LNCaP.<sup>24</sup> Nonetheless, neither the contribution of gankyrin to cancer progression and therapy resistance nor the relationship between gankyrin and TAMs within the TME has been explored in prostate cancer. The present research was therefore conducted to explore the crosstalk and underlying molecular mechanisms between gankyrin and TAMs in prostate cancer progression and ADT resistance.

## Materials and methods

### Cell culture and coculture assays

C4-2B and C4-2 cell lines were generously supplied and authenticated by professor Leland Chung (Cedars-Sinai Medical Center, Los Angeles, California, USA) and cultured in RPMI 1640 medium containing 10% FBS (Gibco, Life

Technologies, Canada) and 1% penicillin–streptomycin solution. U937 cell line, obtained from the Cell Bank of Type Culture Collection of the Chinese Academy of Sciences (Shanghai, China), were maintained in RPMI 1640 medium. All cell lines were cultured at 37°C under a humidified atmosphere of 5% CO<sub>2</sub>. Coculture assays of prostate cancer cells and U937 cells were performed with coculture plates (3421, Corning, USA), as previously described.<sup>9</sup> All the Coculture assays were repeated three times.

### RNA isolation, reverse transcription, and real-time quantitative PCR

For total RNA isolation, cells were suspended in TRIzol® Reagent (Invitrogen, USA), and RNA was extracted according to the protocol. RNA was reverse transcribed to cDNA using the PrimeScript One Step RT reagent kit (Takara Bio, Japan) and quantified with the SYBR Green Real-time PCR Master Mix (TOYOBO, Japan) system using the QuantStudio 6 Flex (Life Technologies, USA) platform. Actin was used as an internal control gene for normalization. The primer sequences are presented in **Supplementary Table S1**. All the real-time quantitative PCR assays were repeated at least three times.

### Patients and specimens

A total of 234 patients who were diagnosed with prostate carcinoma and underwent prostatectomy at Changhai Hospital between 2012 and 2016 were retrospectively recruited for our study. Clinicopathologic data for age, sex, Gleason score, tumor stage and PSA and clinical outcomes were collected. The time to disease progression identified by CT, MRI, or ECT and biochemical recurrence (tPSA = 0.2 ng/mL), were determined as the endpoints for DFS and BCR-free survival, respectively.

All experiments received ethical approval from the Ethics Committee of Changhai Hospital, and all the prostate cancer patients gave their written informed consent. The clinical characteristics of the prostate cancer patients are presented in **Supplementary Tables S2–3**.

### Immunohistochemistry

Paraffin-embedded sections of prostate cancer samples were deparaffinized, rehydrated, and microwaved for 20 min in Tris/EDTA buffer or citric acid buffer to retrieve antigens. Staining was carried out using primary antibodies against the following proteins: Gankyrin (ab182576, Abcam), HMGB1 (ab18256, Abcam), CD68 (M0876, Dako), STAT3 (ab32500, Abcam), p-STAT3 (ab76315, Abcam), and NONO (11058, Proteintech). Samples were scored semiquantitatively according to the percentage of staining intensity and positive cells using the H score (range 0–300), as described previously.<sup>20</sup> All the immunohistochemistry assays were repeated three times.

### Cell viability and apoptosis assays

Cell viability was evaluated via a Cell Counting Kit-8 based on the manufacturer's protocols; Absorbance measurements at 450 nm were taken an EXL800 microplate reader (BioTek Instruments).

For the analysis of cell apoptosis, cells were stained with an Annexin V-FITC/PI apoptosis kit (MULTI SCIENCES, China). Annexin V-positive cells were assessed using a MACSQuant 10 Analyzer (Miltenyi Biotec), and the data were processed with FlowJo software (version 7.6.1; BD Company).

### Cell migration and invasion assay

Cell migration and invasion were assessed by a Transwell system (REF 3422, Corning Incorporated) and Matrigel Invasion Chamber (REF 354480, Corning Incorporated). Briefly, cells were added to the upper chamber containing RPMI 1640 medium without FBS; RPMI 1640 medium containing 40% FBS or conditioned medium (CM) was placed in the lower chamber. The cells were cultured for 3 day, after which the remaining cells in the upper chamber were eliminated. After fixing with 4% paraformaldehyde and staining with crystal violet, the cells on the bottom surface of the membrane were photographed under a microscope.

### Gene knockdown and plasmid transfection

Plasmid transfection and gene knockdown were performed as reported in our previous research.<sup>9</sup> In short,  $5 \times 10^4$  cells/mL prostate cancer cells were added in 6-well plates and transfected with 2  $\mu$ g plasmid containing the overexpression plasmid or empty vector with Lipofectamine<sup>®</sup> 3000 (Invitrogen) according to the manufacturer's protocols. Stable shRNA-mediated gene knockdown was performed by infecting cells with lentivirus expressing shRNA or scrambled control shRNA. The shRNA sequences are shown in **Supplementary Table S1**.

### Western blot and coimmunoprecipitation analyses

Western blot and coimmunoprecipitation analyses were conducted as described in our previous research.<sup>9</sup> Antibodies against the following proteins were used: gankyrin (ab182576, Abcam), HMGB1 (ab18256, Abcam), STAT3 (ab32500, Abcam), p-STAT3 (ab76315, Abcam), NONO (11058, Proteintech), AR (ab74272, Abcam), and GAPDH (#2118S, CST). To analyze gankyrin, HMGB1 and NONO protein interactions, co-immunoprecipitation assays were used with antibodies against the following: gankyrin (ab182576, Abcam), HMGB1 (ab18256, Abcam), and NONO (11058, Proteintech). The GAPDH was utilized as an internal reference.

### Chromatin immunoprecipitation analysis and luciferase reporter assay

Chromatin immunoprecipitation analysis and luciferase reporter assays were performed in our previous study.<sup>9</sup> The following antibodies were applied including AR (ab74272, Abcam) and STAT3 (ab32500, Abcam) antibodies. Rabbit anti-IgG antibodies (2729, CST) served as a negative control. RT-PCR was performed with specific primers flanking the AR-binding site (forward: 5'-TGGAAGCCGAGGAACAGGGTCA-3'; reverse: 5'-GCGTGGAGATGGCAGGGTTAA-3') in the HMGB1 promoter and the STAT3-binding site (forward: 5'-TCCAGAGTGAGGTTTCAGCCTTT-3'; reverse: 5'-

CTCTAGGCCATCCTGCCTTTCT-3') in the gankyrin promoter.

The AR-binding sites of the HMGB1 promoter (sequence: AGGAACAGGGTTCAGC, +1159 to +1173 from the HMGB1 transcription site) and the STAT3-binding sites of the gankyrin promoter (sequence: CTGTTTAGAAA, +177 to +187 from the gankyrin transcription site) or their mutant sequences were cloned into the pGL3-basic luciferase reporter vector; the pRL-TK Renilla luciferase plasmid (Promega, USA) was applied for transfection efficiency normalization. Cells were harvested at 2 day after transfection, and HMGB1 and gankyrin transcription activities were calculated via detecting luminescence with a Dual-Luciferase Assay Kit (Promega, USA). The fold induction value was calculated relative to Renilla luciferase activity.

### RNA sequence

RNA was extracted from C4-2B cells with TRIzol reagent and the total RNA was purified via the Qiagen RNeasy Mini Kit. The specific steps of detection and analysis referred to our previous research (8). The differentially expressed genes regulated by gankyrin in prostate cancer have been listed in **Supplementary Table S7**.

### Immunofluorescence analysis

Prostate cancer cells were placed on round slides and fixed with paraformaldehyde (4%). 0.3% Triton X-100 was applied to permeabilize the cell membrane. Bovine serum albumin (3%) was added to block nonspecific binding prior to the staining procedure. The cells were incubated overnight with antibodies against AR (ab74272, Abcam), HMGB1 (66525-1-Ig, Proteintech), STAT3 (ab32500, Abcam) and gankyrin (sc-101498, Santa Cruz Biotechnology) at 4°C in a humidified chamber. The slides were washed in PBS three times and then incubated for 1 hour using fluorescent dye-conjugated secondary antibodies (4412S and 4409S, 1:1000, CST) at room temperature in a light-proof moisture chamber. Nuclei were visualized by DAPI staining (0.1  $\mu$ g/ml, Servicebio) for 10 min. The slides were then examined and captured using a fluorescence microscope.

### NanoLC-ESI-MS/MS assay

The nanoscale liquid chromatography tandem electrospray ionization mass spectrometry (NanoLC-ESI-MS/MS) assay was carried out as described in our previous study.<sup>9</sup> The proteins identified are listed in **Supplementary Table S8**.

### Antibody-microarray experiment

Cytokine profiles were detected by Quantibody Human Inflammatory Array (RayBiotech) that permitted detection of 40 inflammation-associated cytokines (**Supplementary Table S9-S10**). The specific steps of detection and analysis was carried out as described previously.<sup>9</sup>



## ELISA

HMGB1 and IL-6 concentrations in the cell culture medium were detected by an HMGB1 ELISA Kit (SEA399Hu, Cloud-CloneCorp) and an IL-6 ELISA Kit (SEA079Hu, Cloud-Clone Corp), respectively, following the manufacturer's protocols.

## Animal experiments

A total of  $5 \times 10^6$  C4-2B cells (mixed with Matrigel, 1:1) with the indicated treatment were subcutaneously implanted into the dorsal area between scapulas of 6-week-old male BALB/c nude mice purchased from Shanghai Laboratory Animal Center. In the third week after injection, the mice were surgically castrated and randomly divided into seven groups according to different treatments (Figure 6k; 5 mice/group). The diameter of tumors was measured weekly by a Vernier caliper. Tumor volume was calculated as length  $\times$  width  $\times$  width  $\times$  0.52. All mice were anesthetized with isoflurane and then sacrificed at 7 weeks after inoculation. The animal experimental procedures were received approval from the Animal Care and Use Committee of the Naval Medical University, China.

## Statistical analysis

Numerical variables are presented as the mean  $\pm$  S.D. Continuous variables are expressed as medians (ranges) and categorical variables as numbers (%). Categorical or binary variables were measured by two-tailed Student's *t* test, the chi-squared test or Fisher's exact test and ANOVA for continuous variables. The Kaplan–Meier method and log-rank analysis were applied to plot and compare survival curves, respectively. All experiments were performed independently at least three times. The optimal cutoff values of the gankyrin H-score or CD68 H-score were determined by time-dependent receiver operating characteristic (ROC) analysis. The accuracy of prognostic indicators, including the gankyrin classifier, was investigated by Harrell's concordance index (*c*-index) using the "rms" package in R. The statistical analysis was carried out using GraphPad Prism (version 8.3.0; GraphPad Software), SPSS (version 22.0; IBM Corporation) and R (version 3.6.0). A *p*-value of  $< 0.05$  was considered statistically significant.

## Results

### ***Gankyrin is commonly upregulated in prostate cancer and predicts unfavorable prognosis***

To determine the expression of gankyrin in prostate cancer, the Gene Expression Omnibus (GEO) and ONCOMINE databases<sup>25</sup> were first utilized to demonstrate that prostate cancer tissues had higher expression levels of gankyrin than normal tissues (Supplementary Fig. S1A–B). Consistent with the above findings, immunohistochemistry assays showed upregulated gankyrin expression in localized prostate cancer, androgen deprivation therapy (ADT)-treated, and castration-resistant prostate cancer (CRPC) tissues, in contrast to benign prostate hyperplasia (BPH) tissues (Figure 1a). Additionally, stronger gankyrin expression was observed in specimens with Gleason scores  $> 7$  than in tissues with Gleason scores  $< 7$

(Figure 1b). Immunohistochemistry staining revealed higher gankyrin expression in poorly differentiated areas, even in the same sample (Figure 1b). Moreover, higher levels of gankyrin were observed in ADT-treated patient specimens than in the corresponding tissues of the same patient before ADT (Figure 1c). Consistently, gankyrin expression was higher in ADT-treated orthotopic xenografts or cell lines of prostate cancer than in naïve samples or cells from the patients who received no ADT treatment before operation (Supplementary Fig. S1C–F). These data suggest that increased gankyrin expression is correlated with prostate cancer progression and ADT resistance.

Moreover, we assessed the relationship between gankyrin expression and the clinical outcomes of prostate cancer patients. A total of 234 prostate cancer patients were randomly separated into two cohorts at a 1:1 ratio: a training cohort ( $n = 117$ ) and a validation cohort ( $n = 117$ ). Gankyrin expression was determined by the H-score (Figure 1d). The best cutoff values for allocating patients into the high or low expression groups were determined by receiver operating characteristic analysis, which demonstrated that the optimal cutoff value was 135.5, with an AUC of 0.724, via biochemical recurrence (BCR) as the end point in the training cohort ( $n = 117$ , Figure 1e). Concordantly, high expression of gankyrin indicated higher PSA levels, Gleason scores, and T stage in the training cohort (Supplementary Table S2). Based on Kaplan–Meier survival analysis, patients in the training cohort with high gankyrin expression had markedly worse BCR and DFS than those with low gankyrin expression (figure 1f–g); these results were validated with the validation cohort utilizing the cutoff value derived from the training cohort (Supplementary Table S3; Figure 1h–i). To further assess the prognostic value of gankyrin, univariate and multivariate Cox regression analyses were applied to determine whether gankyrin can serve as an independent risk factor for BCR and DFS in prostate cancer patients. Even after multivariable adjustment by clinical characteristics, gankyrin appeared to be an independent risk factor for BCR and DFS in both cohorts (Supplementary Tables S4–S5). Analysis of Harrell's *c*-index showed that gankyrin combined with the Gleason score, TNM stage or PSA resulted in a higher *c*-index value than gankyrin or other predictors alone for BCR or DFS in both cohorts (Supplementary Table S6), indicating that gankyrin may constitute a valuable indicator of prostate carcinoma prognosis.

### ***Gankyrin promotes the malignant features of prostate cancer in vitro and in vivo***

To determine whether gankyrin regulates the progression of prostate cancer, gankyrin expression was stably silenced in prostate carcinoma cell lines; as expected, the knockdown of gankyrin suppressed the invasion and migration abilities of prostate cancer cells (Figure 2a and b, Supplementary Fig. S2A–C). Additionally, gankyrin-knockdown C4-2B and C4-2 cells exhibited more apoptosis and had decreased survival ability compared with control cells when exposed to the ADT drug enzalutamide (Figure 2c and d, Supplementary Fig. S2D–E). Moreover, in a subcutaneous tumorigenesis model, xenografts derived from C4-2B cells with gankyrin knockdown had

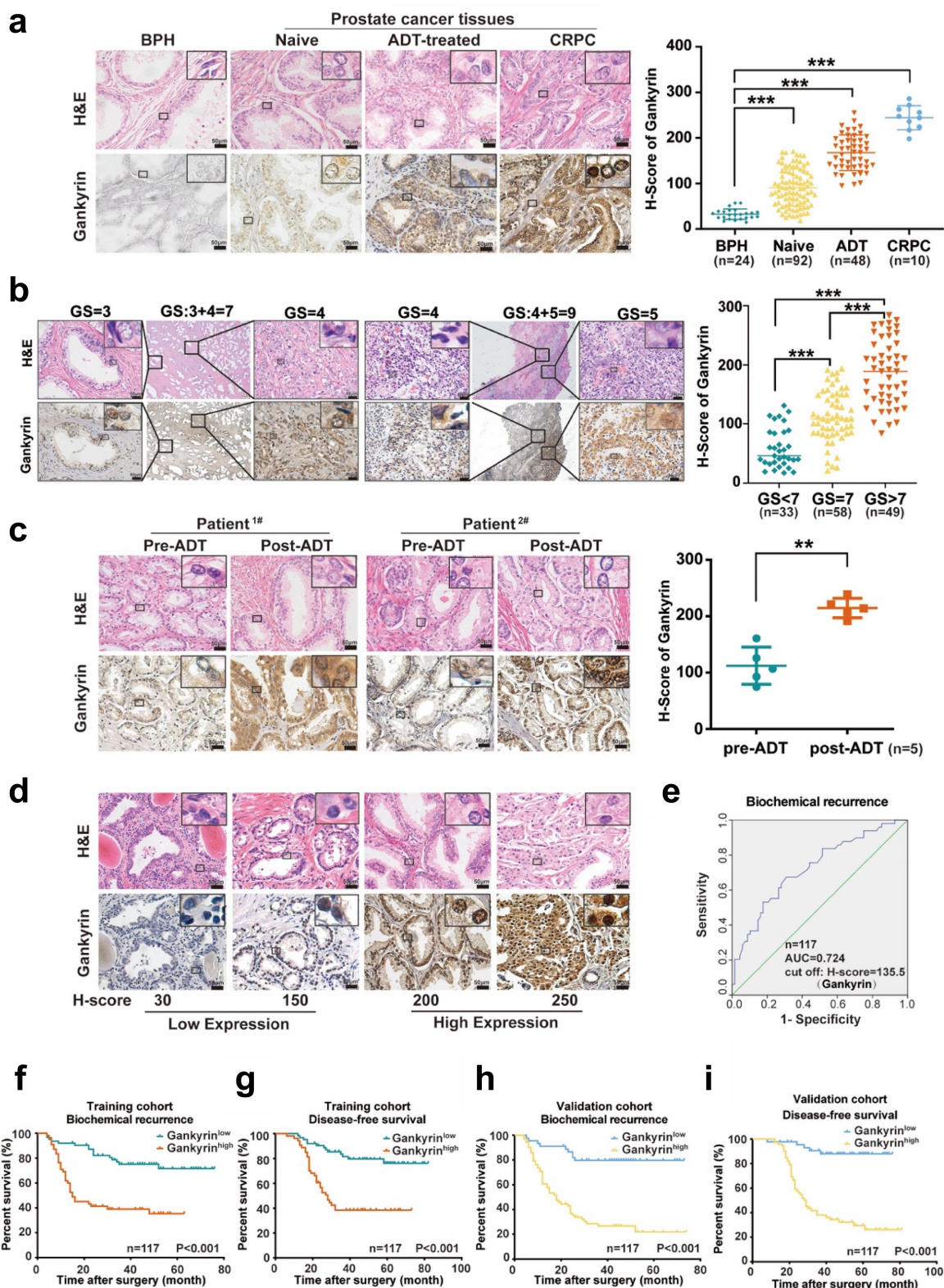


**Figure 1.** Gankyrin is commonly upregulated in prostate cancer and predicts unfavorable prognosis. **(a)**, Representative immunohistochemistry (IHC) images for gankyrin in BPH tissues and localized prostate cancer, androgen deprivation therapy (ADT)-treated, or castration-resistant prostate cancer (CRPC) tissues. H-scores of gankyrin expression in different groups are shown. **(b)**, Immunohistochemistry images of gankyrin in samples with corresponding Gleason Scores (GSs). H-scores of gankyrin expression in different samples are shown. **(c)**, Pre-ADT and post-ADT tissues are from the same patient who received ADT. H-scores for gankyrin in the two groups are shown (right). **(d)**, Representative images of gankyrin expression in prostate cancer tissues (Scale bar in A-D = 50  $\mu$ m). **(e)**, A time-dependent receiver operating characteristic analysis was calculated to calculate the optimum cutoff value of gankyrin (H-score) to predict biochemical recurrence (BCR) in the training cohort. **(f-g)**, Kaplan–Meier curves of BCR (f) and DFS (g) were plotted based on gankyrin expression in the training cohort. **(h-i)**, Kaplan–Meier curves for BCR (h) and DFS (i) of prostate cancer patients were plotted based on gankyrin expression in the validation cohort (\*\*p < .01 and \*\*\*p < .001).



weaker growth ability than those derived from control cells (Figure 2e and f).

To validate the function of gankyrin in prostate cancer, we generated C4-2B and C4-2 cells stably overexpressing gankyrin (Supplementary Fig. S2F). In contrast to the results for gankyrin knockdown, overexpression of gankyrin enhanced the invasion, migration, enzalutamide resistance, and tumorigenicity of prostate cancer cells (Figure 2g–i, Supplementary Fig. S2G–J). Collectively, the results suggest that gankyrin facilitates the biological characteristics of prostate cancer.

### **HMGB1 is indispensable for gankyrin-induced cell migration, invasion, and ADT resistance in prostate cancer**

To investigate the mechanism underlying gankyrin-regulated biological characteristics of prostate cancer cells, RNA sequencing of C4-2B cells with gankyrin (*PSMD10*) knockdown and C4-2B cells was performed, and the results identified the differentially expressed genes and cell signaling regulated by gankyrin (Figure 3a, Supplementary Fig. S3A–B, and Table S7). Among these differentially expressed genes, we paid much attention to high-mobility group protein box 1 (HMGB1) because our previous study demonstrated that HMGB1 plays significant roles in inducing ADT resistance and that high expression of HMGB1 indicates poor prognosis in prostate cancer patients.<sup>9</sup> As expected, higher expression of HMGB1, similar to that of gankyrin, was found in ADT-treated prostate cancer tissues than in pre-ADT tissues (Figure 3a). Additionally, gankyrin expression was positively associated with HMGB1 expression in prostate cancer tissues (Figure 3b and c). Thus, we examined whether gankyrin mediates HMGB1 effects in prostate cancer. First, the expression and secretion of HMGB1 were generally consistent with those of gankyrin in prostate cancer cells with gankyrin knockdown or overexpression (Figure 3d–g; Supplementary Fig. S3C–D). Second, stable HMGB1-depleted C4-2B and C4-2 cells were constructed, and as anticipated, suppression of HMGB1 weakened the migration and invasion abilities enhanced by gankyrin overexpression in these prostate cancer cells (Figure 3h; Supplementary Fig. S3E–F). Moreover, HMGB1 inhibition restored sensitivity to enzalutamide in C4-2B and C4-2 cells overexpressing gankyrin (Figure 3i–j; Supplementary Fig. S3E–F). These findings demonstrate that HMGB1 is a necessary downstream mediator of gankyrin signaling in prostate cancer for regulating progression and ADT resistance.

### **Gankyrin activates the NONO-AR-HMGB1 signaling pathway responsible for prostate cancer progression**

We further examined how gankyrin regulates HMGB1 in prostate cancer. Given that gankyrin is not a transcription factor, we hypothesized that the interaction between these proteins might be regulated by an indirect mechanism. Hence, the gankyrin protein was immunoprecipitated with an anti-gankyrin antibody followed by nanoscale liquid chromatography tandem electrospray ionization mass spectrometry (Nano LC–ESI–MS/MS). Among the gankyrin-interacting

proteins identified (Figure 4a, Supplementary Table S8), non-POU-domain-containing octamer-binding protein (NONO) has been reported to promote carcinogenesis and progression of breast cancer, hepatocellular carcinoma and prostate cancer.<sup>26</sup> Coimmunoprecipitation (co-IP) assays were also performed to identify a direct interaction between gankyrin and NONO in prostate cancer cells (Figure 4b). In addition, gankyrin knockdown elicited a robust decrease in the mRNA level of NONO, as revealed by RNA-sequencing data or real-time PCR assays (Figures 3a and 4c; Supplementary Fig. S4A), whereas the overexpression of gankyrin led to the opposite effect (Figure 4c; Supplementary Fig. S4A). NONO was also found among HMGB1-interacting proteins by Nano LC–ESI–MS/MS in one of our previous works,<sup>9</sup> as confirmed by coimmunoprecipitation in the present study (Figure 4d). To further explore whether NONO is involved in HMGB1 expression regulation by gankyrin, NONO was knocked down in prostate carcinoma cells (Supplementary Fig. S4B). As presented in Figure 4e, gankyrin-upregulated HMGB1 expression was alleviated by NONO knockdown. NONO was also overexpressed in prostate cancer cells (Supplementary Fig. S4C), and as expected, NONO overexpression attenuated the decrease in HMGB1 expression in prostate cancer cells caused by gankyrin knockdown (Figure 4f).

Although NONO interacts with both HMGB1 and gankyrin, no transcription factor-binding site for NONO was found in the HMGB1 promoter through online JASPAR software. Thus, we speculate that another transcription factor regulated by NONO is involved in the regulation of HMGB1 expression. Previous research has established that NONO promotes androgen receptor (AR) and variant splicing and expression at the mRNA and protein levels in prostate cancer.<sup>26</sup> To substantiate these results, we observed that NONO knockdown triggered a decrease in AR expression but that NONO overexpression had the opposite effect (Figure 4g). Moreover, the most universal mechanism driving progression and ADT resistance appears to be reactivation of the AR signaling pathway mediated by high levels of AR or its variants in prostate cancer.<sup>27</sup> Therefore, we suspect that the transcription factor AR plays a role in regulating HMGB1 expression. In agreement, we observed that AR knockdown, consistent with NONO knockdown, significantly suppressed the elevation in HMGB1 expression and secretion due to gankyrin overexpression in prostate cancer cells (Figure 4h–i; Supplementary Fig. S4D). Furthermore, gankyrin overexpression led to stronger AR and HMGB1 immunofluorescence staining intensity in C4-2B cells, which was dramatically attenuated by either NONO or AR knockdown (Supplementary Fig. S4E). We further investigated whether AR was needed to regulate HMGB1 transcription, and online JASPAR software was used to determine putative AR-binding sites in the HMGB1 promoter (Supplementary Fig. S4F). As shown in Figure 4j, a chromatin immunoprecipitation (ChIP) assay revealed that AR bound to the HMGB1 promoter in C4-2B cells, and this binding was enhanced by gankyrin overexpression. Although gankyrin overexpression enhanced HMGB1 transcriptional activity, mutated versions of the AR-binding sites in the HMGB1 promoter did not show this effect (Figure 4k). These findings collectively demonstrate that

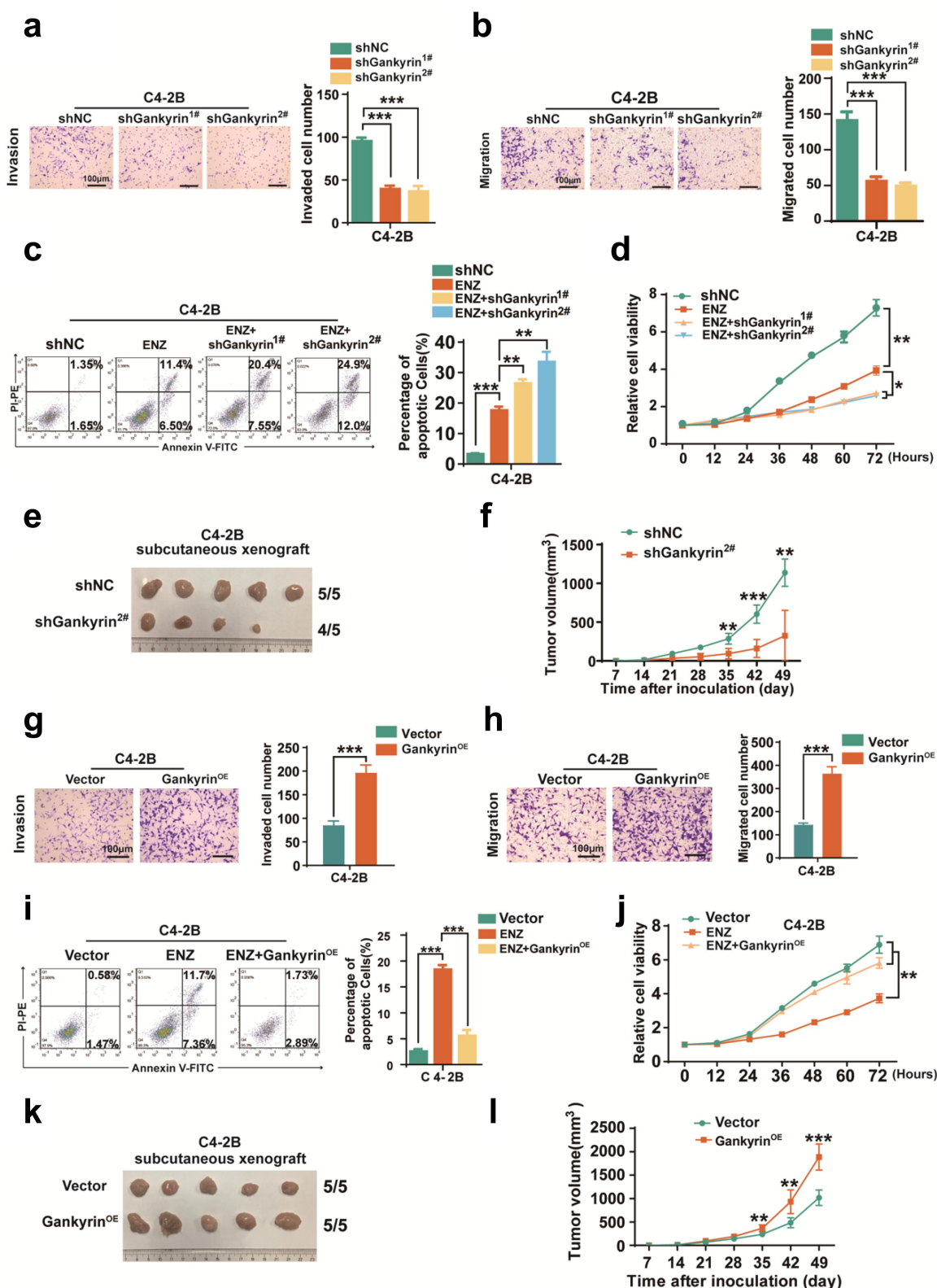


**Figure 2.** Gankyrin promotes the malignant features of prostate cancer. **(a-b)**, Invasion (a) and migration (b) analyses were taken in C4-2B cells with or without gankyrin knockdown (scale bar = 100  $\mu$ m). Quantification of invaded or migrated cells in the two groups is shown (right). **(c-d)**, Apoptosis (c) and cell viability (d) analyses were performed in naïve C4-2B cells and enzalutamide-treated cells without or with gankyrin knockdown. **(e-f)**, C4-2B cells with gankyrin knockdown and control cells were subcutaneously injected into nude mice (n = 5/group). Visual examination of isolated tumors from the two groups (e) and statistical analysis of tumor volume in the indicated groups after inoculation (f) are presented. **(g-h)**, Invasion (g) and migration (h) analyses were taken in C4-2B cells with or without gankyrin overexpression (scale bar = 100  $\mu$ m). Quantification of invaded or migrated cells in the two groups is shown (right). **(i-j)**, Apoptosis (i) and cell viability (j) analyses were performed in naïve C4-2B cells and enzalutamide-treated C4-2B cells without or with gankyrin overexpression. **(k-l)**, Gankyrin-overexpressing C4-2B cells and control cells were subcutaneously injected into nude mice (n = 5/group). Visual examination of isolated tumors from the two groups (k) and statistical analysis of tumor volume in the indicated groups after inoculation (l) are presented (\*p < .05, \*\*p < .01, and \*\*\*p < .001).

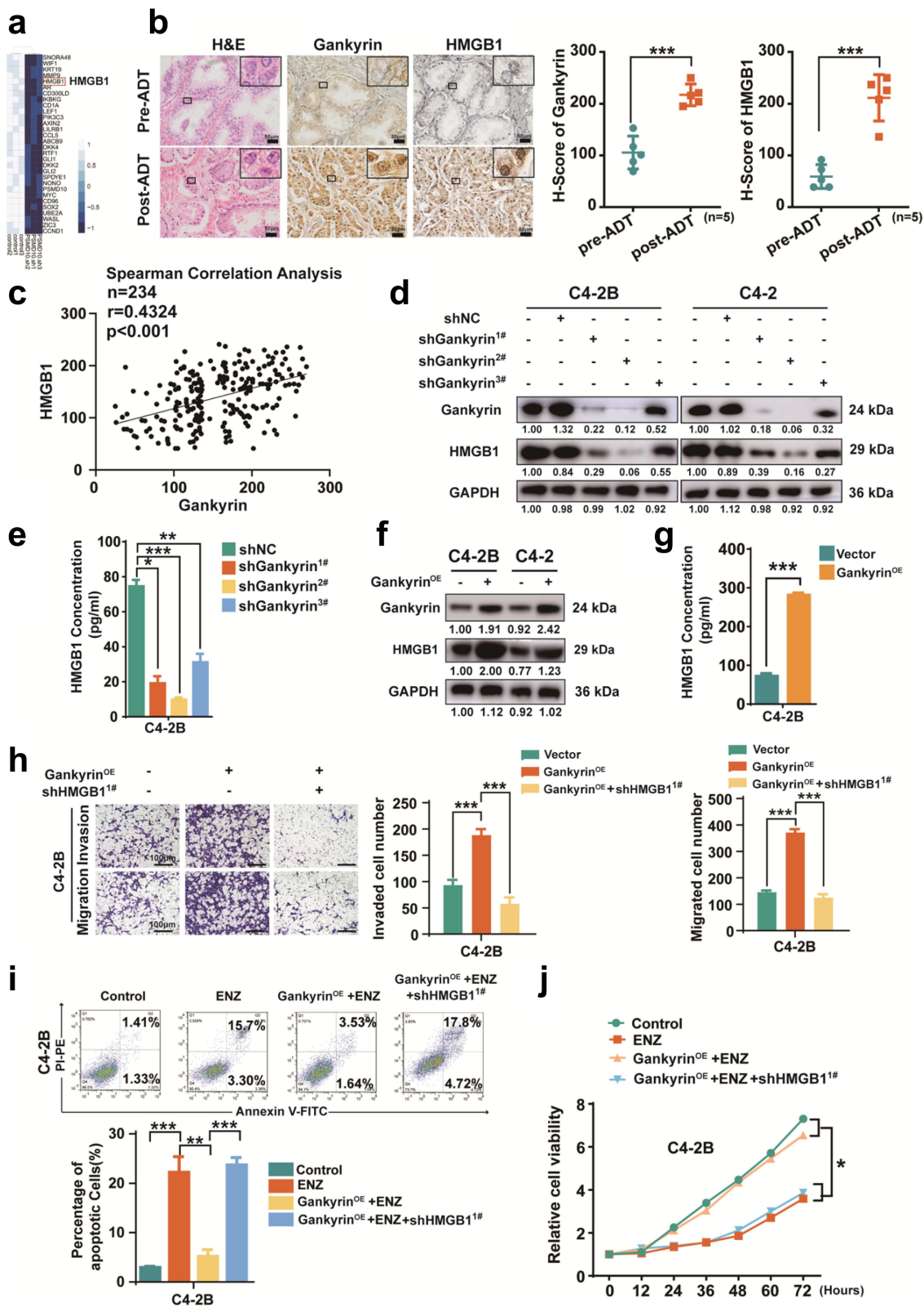


**Figure 3.** HMGB1 is indispensable for gankyrin-induced cell migration, invasion, and ADT resistance in prostate cancer. **(a)**, RNA-seq was performed, and a heatmap revealing the markedly differentially expressed genes in C4-2B cells without or with gankyrin knockdown are presented. **(b)**, Representative images and statistical analysis of gankyrin and HMGB1 expression in pre-ADT and post-ADT prostate cancer samples (scale bar = 50  $\mu$ m). **(c)**, Spearman correlation analysis of gankyrin and HMGB1 in prostate cancer samples. **(d)**, Western blotting assay of gankyrin and HMGB1 expression in control (shNC) and gankyrin-knockdown (shgankyrin) C4-2B or C4-2 cells. **(e)**, Quantification of HMGB1 protein in culture media of control and gankyrin-knockdown C4-2B cells by ELISA. **(f)**, Western blotting assay of gankyrin and HMGB1 protein expression in gankyrin-overexpressing (Gankyrin<sup>OE</sup>) or control C4-2B and C4-2 cells. **(g)**, Quantification of HMGB1 protein in culture media of control and gankyrin-overexpressing C4-2B cells by ELISA. **(h)**, Representative micrographs and quantification of the invasion and migration abilities of C4-2B cells and gankyrin-overexpressing C4-2B cells without or with HMGB1 knockdown (shHMGB1) (scale bar = 100  $\mu$ m). **(i-j)**, Apoptosis **(i)** and cell viability **(j)** analyses were performed in naive C4-2B cells, enzalutamide-treated C4-2B cells, and enzalutamide-treated gankyrin-overexpressing C4-2B cells without or with HMGB1 knockdown (\* $p$  < .05, \*\* $p$  < .01 and \*\*\* $p$  < .001).



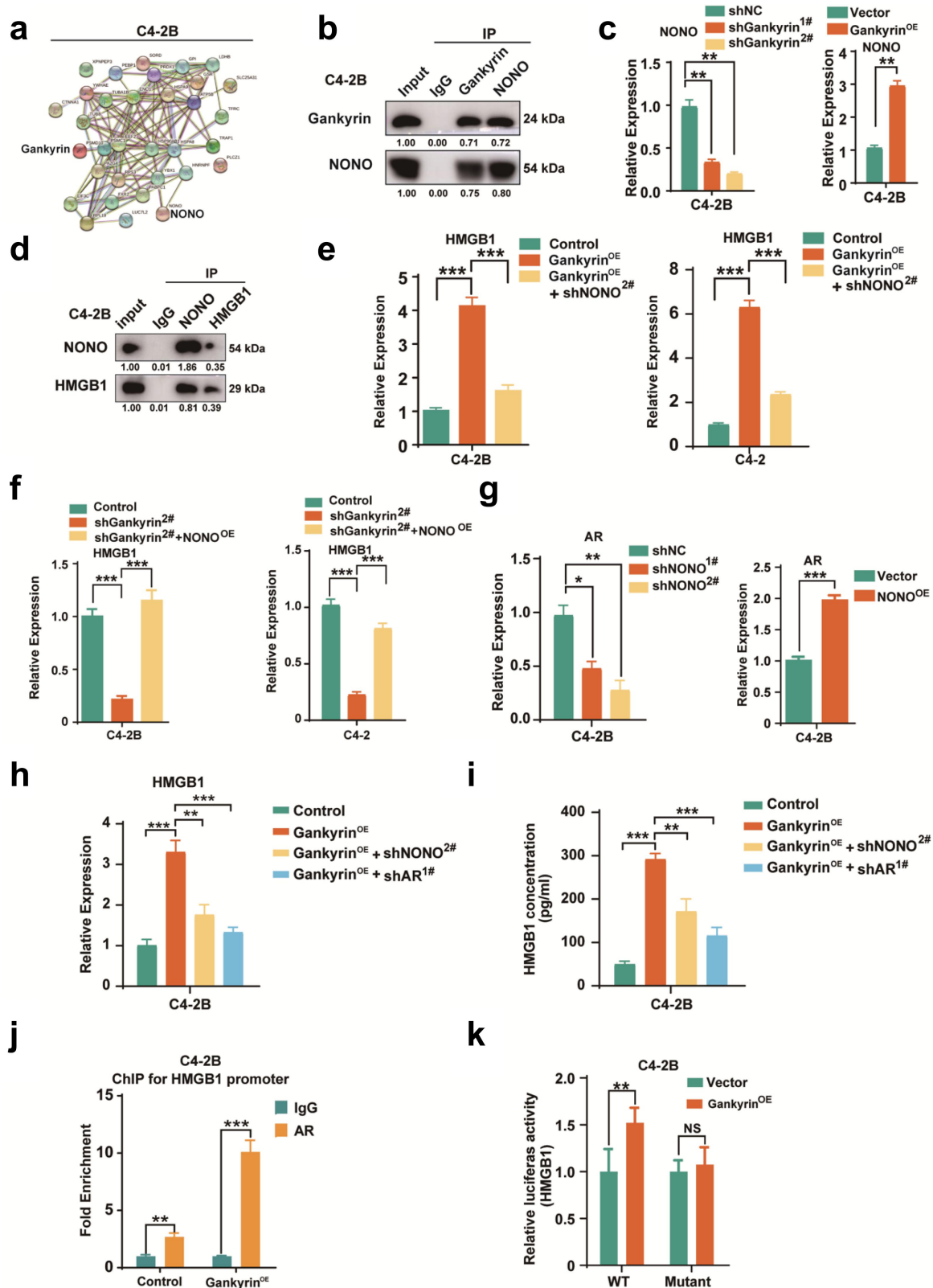


**Figure 4.** Gankyrin activates the NONO-AR-HMGB1 signaling pathway responsible for prostate cancer progression. **(a)**, Gankyrin-interacting proteins validated by Nano LC-ESI-MS/MS and the protein-protein interaction network (STRING database) are presented. **(b)**, Western blot analysis was utilized to identify endogenous gankyrin Co-immunoprecipitated (Co-IP) with NONO in C4-2B. IgG was detected as a control for Co-IP. **(c)**, NONO mRNA expression was detected by RT-PCR in gankyrin-knockdown (shGankyrin, left) or gankyrin overexpression (Gankyrin<sup>OE</sup>, right) C4-2B cells and control cells. **(d)**, Western blot analysis was utilized to identify endogenous NONO Co-immunoprecipitated with HMGB1 in C4-2B. **(e)**, Real-time PCR assays of HMGB1 expression in gankyrin-overexpressing prostate cancer cells with or without NONO knockdown. **(f)**, RT-PCR assays of HMGB1 expression in gankyrin knockdown prostate cancer cells without or with NONO overexpression. **(g)**, AR expression was detected by real-time PCR in NONO-knockdown (shNONO, left) and NONO-overexpressing (NONO<sup>OE</sup>, right) C4-2B cells. **(h)**, HMGB1 expression was detected by real-time PCR in control cells, gankyrin-overexpressing C4-2B without or with NONO or AR knockdown. **(i)**, Quantification of the HMGB1 protein was performed in the culture media of control cells, gankyrin-overexpressing C4-2B without or with NONO or AR knockdown. **(j)**, ChIP assay was taken to determine binding of AR to the HMGB1 promoter in control cells and gankyrin-overexpressing C4-2B. **(k)**, Binding of AR to the HMGB1 promoter was confirmed by luciferase analyses in control cells and gankyrin-overexpressing C4-2B. AR binding was hindered in reporter gene with mutated variants (\*\* $p < .01$  and \*\*\* $p < .001$ ).

gankyrin mediates HMGB1 transcription and expression via NONO/AR in prostate cancer.

### ***Gankyrin facilitates prostate cancer progression via interaction between tumor cells and tumor-associated macrophages (TAMs)***

Numerous studies, including ours, have demonstrated that to effectively hinder tumor progression, researchers should pay attention not only to tumor cells but also to the TME interacting with these cells.<sup>13,28,29</sup> Consistently, the levels of the TAM marker CD68 were elevated in ADT-treated prostate carcinoma samples compared with naïve tissues, and the results were generally consistent with those found for gankyrin and HMGB1 expression (Figure 5a, Supplementary Fig. 5A). In addition, Spearman correlation analysis revealed that gankyrin expression was positively associated with CD68 expression in prostate cancer tissues (Figure 5b). Moreover, prostate cancer patients in both the training and validation cohorts harboring high expression of gankyrin and CD68 exhibited the worst BCR and DFS (Figure 5c and d; Supplementary Fig. S5C-D).

We then examined whether gankyrin/HMGB1/NONO/AR facilitates the progression of prostate cancer by promoting the interaction between prostate cancer cells and TAMs. First, the number of migrating U937 cells (a TAM cell line) exposed to conditioned medium (CM) from prostate cancer cells was much greater than that from control U937 cells (Figure 5e; Supplementary Fig. S5E). The number of migrated U937 cells was further increased when U937 cells were exposed to CM from prostate cancer cells overexpressing gankyrin (Figure 5e; Supplementary Fig. S5E). However, the increase in U937 cells due to gankyrin was abolished by NONO knockdown or treatment with an HMGB1-neutralizing antibody (Figure 5e; Supplementary Fig. S5E). In addition, a significant reduction in the expression of M1 phenotype genes (CD80, CD86, TLR-4) and a significant increase in M2 phenotype genes (CD163, ARG1, IL-10) were observed in U937 cells exposed to CM from prostate cancer cells compared with control U937 cells (Figure 5f and g; Supplementary Fig. S5F). Overexpression of gankyrin in prostate cancer cells further reduced M1 phenotype gene expression and increased M2 phenotype gene expression in U937 cells, but NONO knockdown or an HMGB1-neutralizing antibody alleviated these effects (Figure 5f and g; Supplementary Fig. S5F). The above results indicate that gankyrin overexpression can initiate the recruitment and M2 polarization of TAMs via NONO/HMGB1.

We then employed a coculture system to investigate whether gankyrin/NONO/HMGB1-activated TAMs have an impact on the migration and invasion of prostate carcinoma cells. Cocultured gankyrin-overexpressing C4-2B cells exhibited stronger invasion and migration abilities than C4-2B cells cultured with U937 alone or C4-2B cells, and supplementation with NONO shRNA or an HMGB1-neutralizing antibody abrogated this effect (Figure 5h, Supplementary Fig. S5G). Gankyrin overexpression and coculture with U937 cells also exerted a synergistic effect on enzalutamide resistance in prostate cancer cells, whereas NONO shRNA or an HMGB1-neutralizing antibody, as anticipated, abolished this synergistic effect (Figure 5i, Supplementary Fig. S5H). In summary, these

data indicate that gankyrin/HMGB1/NONO/AR promotes the progression of prostate cancer by facilitating the interaction between prostate cancer cells and TAMs.

### ***Blocking the positive regulatory loop gankyrin/NONO/AR/HMGB1/IL-6/STAT3 inhibits ADT resistance in prostate cancer***

We subsequently examined how HMGB1-induced TAMs regulate ADT resistance in prostate carcinoma. First, to detect the cytokines derived from HMGB1-associated TAMs, a RayBio Human Cytokine Antibody Array was performed to identify the cytokine profiles in the culture medium from U937 or cocultured with C4-2B in the absence or addition of an HMGB1-neutralizing antibody (HMGB1 ab, Figure 6a-c, Table S9-S10). The CM from U937 cells cocultured with C4-2B cells presented significantly upregulated levels of seven cytokines in contrast to that from U937 cells cultured alone. In addition, compared with the CM from cocultured U937/C4-2B cells, the CM from cocultured U937 cells with HMGB1 ab displayed six differentially downregulated cytokines (Figure 6a and b, Table S9). The significantly differentially expressed cytokines were then compared via a Venn plot, which revealed that IL-6 was the critical cytokine (Figure 6c, Table S10). As expected, the secretion and transcription of IL-6 were elevated in U937 cells cocultured with C4-2B cells in contrast to U937 cells alone; HMGB1 inhibition via an HMGB1 ab reduced the above effects (Figure 6d and e). Elevated levels of p-STAT3 (Y705) in C4-2B cells cocultured with U937 cells were abolished by an HMGB1 ab, whereas recombinant human IL-6 restored the reduced phosphorylation levels of STAT3 (Figure 6f). These results suggest that IL-6/STAT3 is necessary for HMGB1-induced TAM-mediated regulation of ADT resistance.

Given that gankyrin expression was elevated after ADT treatment in prostate cancer tissues and prostate cancer cells (Figure 1a, Supplementary Fig. S1C-F), we next asked whether TAM-activated IL-6/STAT3 signaling induces the expression of gankyrin during ADT resistance in prostate carcinoma. First, C4-2B cells cocultured with U937 cells exhibited higher gankyrin expression than control cells cultured alone, and this increase was retarded by IL-6 ab or STAT3 knockdown (Figure 6g, Supplementary Fig. S6A). Second, the results of immunofluorescence staining revealed that in contrast to C4-2B, the coculture of C4-2B and U937 led to stronger STAT3 and gankyrin expression but that an IL-6-neutralizing antibody or STAT3 knockdown attenuated these effects (Supplementary Fig. S6B). Third, ChIP assays indicated that STAT3 bound to the gankyrin promoter in C4-2B cells, and this binding was enhanced after C4-2B cells were cocultured with U937 cells (Figure 6h, Supplementary Fig. S6C). In luciferase assays, STAT3 binding to the gankyrin promoter was blocked by utilizing reporter constructs harboring mutated versions, which abolished the enhanced transcriptional activity of gankyrin after the coculture of C4-2B cells with U937 cells (Figure 6i). These results collectively demonstrate that HMGB1-activated TAMs promote gankyrin transcription via IL-6/STAT3 signaling, creating a positive feedback loop with the gankyrin/NONO/AR/HMGB1/IL-6/STAT3 axis. Moreover, higher expression of gankyrin, NONO, HMGB1,

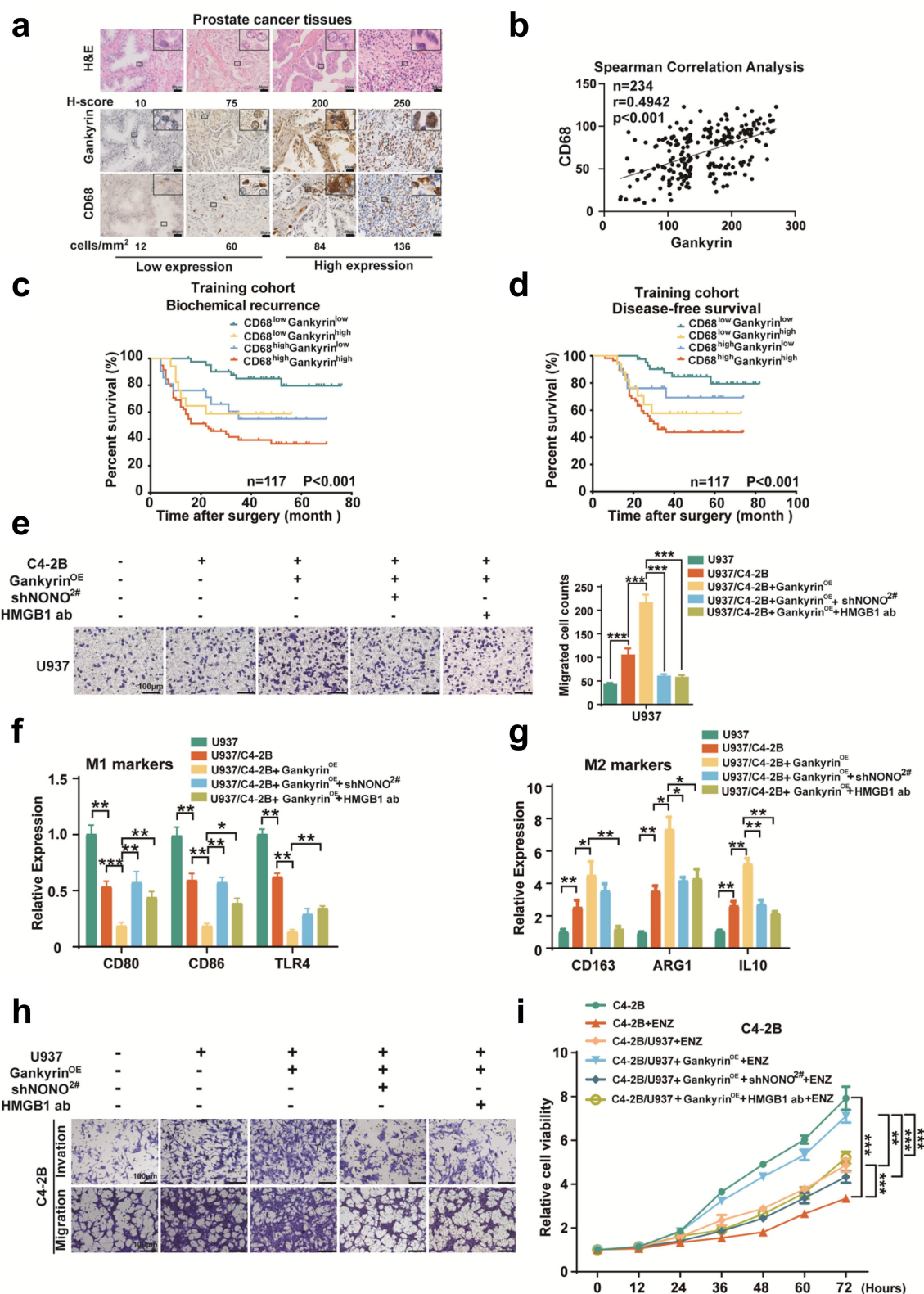


**Figure 5.** Gankyrin facilitates prostate cancer progression via interaction between tumor cells and tumor-associated macrophages (TAMs). **(a)**, Immunohistochemistry and H&E images of gankyrin and CD68 expression in prostate carcinoma samples (scale bar = 50  $\mu$ m). **(b)**, Spearman Correlation analysis of gankyrin and CD68 in prostate carcinoma samples. **(c-d)**, Kaplan-Meier curves of BCR and DFS in prostate carcinoma patients in the training cohort were analyzed. **(e)**, Pictures and counts of migrated U937 cells cultured in conditioned medium of cocultured C4-2B cells or gankyrin-overexpressing (Gankyrin<sup>OE</sup>) C4-2B without or with NONO knockdown or treated with an HMGB1-neutralizing antibody (scale bar = 100  $\mu$ m). **(f-g)**, Real-time PCR was performed to analyze the expression of M1 (f) or M2 (g)-related genes in U937 cells cocultured with control C4-2B and gankyrin-overexpressing C4-2B with or without NONO knockdown or treated with an HMGB1-neutralizing antibody. **(h)**, Representative micrographs of the invasion and migration abilities of C4-2B cultured alone or with U937 cells, with or without gankyrin overexpression in the absence or exist of NONO knockdown or treated with an HMGB1-neutralizing antibody (scale bar = 100  $\mu$ m). **(i)**, Cell viability analysis was performed in naive C4-2B cells, enzalutamide-treated C4-2B, and enzalutamide-treated gankyrin-overexpressing C4-2B cultured alone or with U937 cells in the absence or exist of NONO knockdown or treated with an HMGB1-neutralizing antibody (\* $p$  < .05, \*\* $p$  < .01 and \*\*\* $p$  < .001).



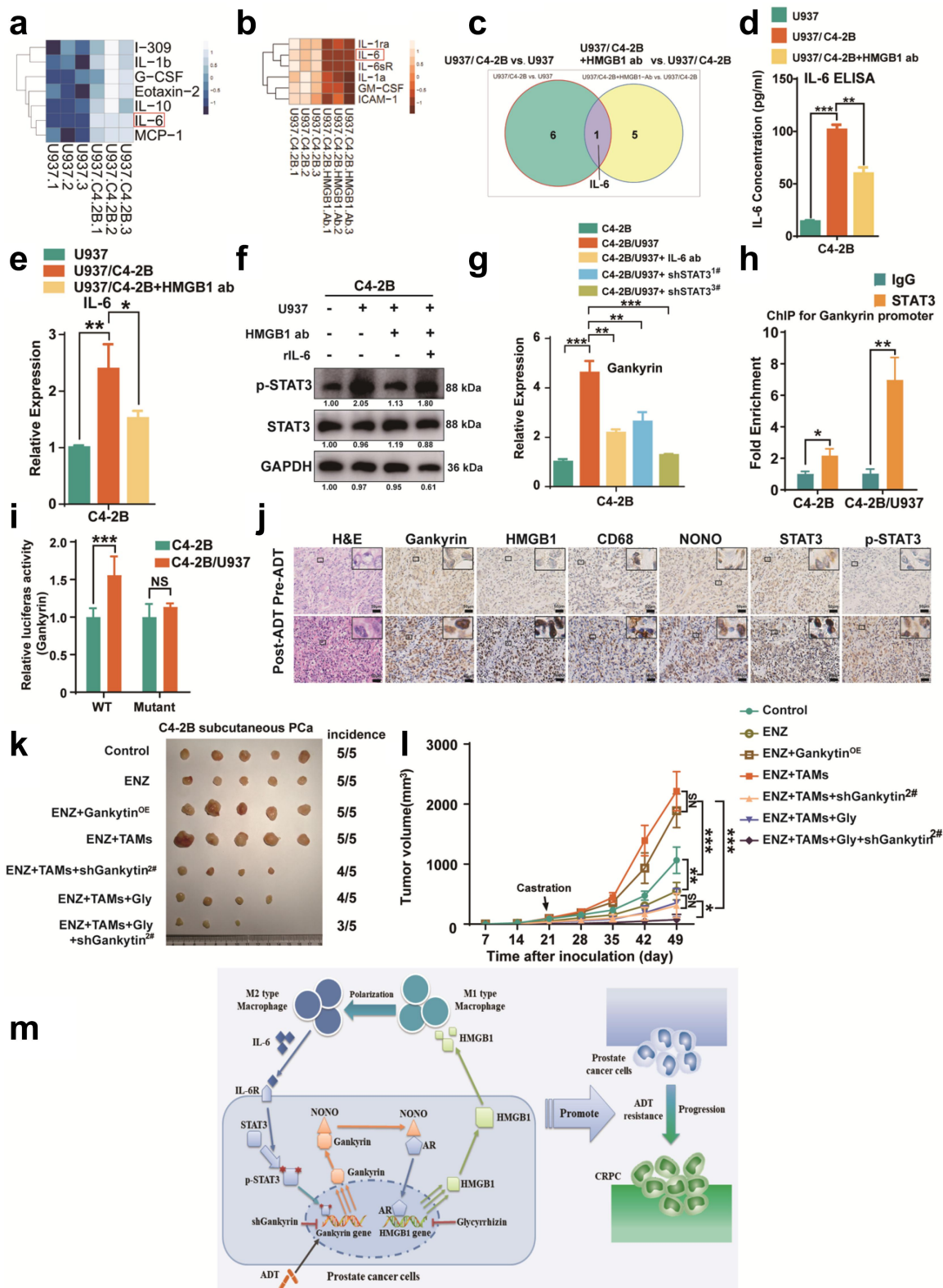


**Figure 6.** Blocking the positive regulatory loop gankyrin/NONO/HMGB1/IL-6/STAT3 inhibits ADT resistance in prostate cancer. **(a)** The RayBio Human Cytokine Antibody Array was performed to analyze the Cytokine profiles. Heatmap revealing the differentially expressed cytokines in conditioned medium of U937 cells cultured alone or with C4-2B cells. **(b)** Heatmap revealing the differentially expressed cytokines in CM U937 cells cocultured with C4-2B cells alone or with HMGB1 Ab. **(c)** A Venn plot of differentially expressed cytokines is presented. **(d)** Quantification of IL-6 protein secretion in culture media of U937 or cocultured with C4-2B in the absence or presence of HMGB1. **(e)** IL-6 expression was detected via RT-PCR in U937 cells or cocultured with C4-2B in the absence or presence of HMGB1 ab. **(f)** Western blotting assay was utilized to evaluate the expression of STAT3 and p-STAT3 (Y705) in C4-2B or cocultured with U937 cells in the absence or presence of HMGB1 ab and rIL-6. **(g)** Gankyrin expression was evaluated via real-time PCR in C4-2B or cocultured with U937 cells in the absence or presence of IL-6 ab or shSTAT3. **(h)** ChIP assay was performed to detect the binding of STAT3 to the gankyrin promoter in C4-2B cocultured with U937 cells. **(i)** Binding of STAT3 to the gankyrin promoter was confirmed by luciferase analyses in C4-2B cultured alone or with U937 cells. STAT3-binding sites were hindered in reporter gene with mutated version. **(j)** Representative H&E and immunohistochemistry micrographs for gankyrin, HMGB1, CD68, NONO, STAT3, and p-STAT3 expression in pre-ADT and post-ADT prostate cancer tissues (scale bar = 50  $\mu$ m). **(k-l)** C4-2B or cocultured with U937 in the absence or presence of enzalutamide (ENZ), HMGB1 inhibitor glycyrrhizin (Gly) or gankyrin-targeting shRNA

STAT3, p-STAT3 and the TAM marker CD68 was detected in ADT-treated prostate carcinoma samples than in corresponding pre-ADT samples (Figure 6j; Supplementary Fig. S6D-I).

Next, we examined whether blocking the feedback loop using gankyrin shRNA or the HMGB1 inhibitor glycyrrhizin (Gly) enhanced the therapeutic effect of ADT in a xenograft model of prostate cancer. Enzalutamide inhibited the growth of C4-2B-derived tumors but had little effect on the growth of tumors from gankyrin-overexpressing C4-2B cells or C4-2B cells cocultured with U937 cells (Figure 6k and l). However, gankyrin knockdown or glycyrrhizin restored the sensitivity of C4-2B cells cocultured with U937 cells to enzalutamide, and the combination of gankyrin knockdown and glycyrrhizin with enzalutamide further inhibited the growth of C4-2B-U937 cell-derived tumors in the subcutaneous xenograft mouse model (Figure 6k and l).

## Discussion

While prostate cancer cells initially respond to ADT with various durations, nearly all prostate cancer patients will ultimately experience resistance to anti-androgen agents, either first-generation or second-generation antiandrogens, resulting in inevitable progression to CRPC, the lethal form of prostate cancer.<sup>30</sup> The development of ADT resistance remains a major challenge for the treatment of advanced-stage prostate cancer, with limited effective treatment choices for patients. Further research is urgently needed to find a way to slow tumor progression and reduce therapy resistance. In this study, blocking gankyrin/NONO/AR/HMGB1/IL-6/STAT3 signaling by gankyrin silencing or the HMGB1 inhibitor glycyrrhizin, which disturbed the positive feedback loop between prostate cancer cells and TAMs, effectively restored the sensitivity of these cells to enzalutamide *in vitro* and *in vivo* (Figure 6m). Therefore, combined inhibition of both gankyrin signaling and TAMs may be an effective way to prolong the duration of response to ADT in prostate cancer.

Although the AR-independent noncanonical pathway is the most widely accepted mechanism driving CRPC development with respect to consistent restoration of AR-dependent canonical signaling mediated by high levels of AR and AR splice variants in prostate cancer, it also plays critical roles in the development of therapy resistance. Notably, increased glucocorticoid receptor (GR) expression occurs in enzalutamide-resistant tumors and is related to resistance to ARN-509, a second-generation antiandrogen.<sup>5</sup> During the development of neuroendocrine prostate cancer, the GR/MYC/N/CDK5/RB1/E2F1 signaling bypass can function independently of AR to facilitate the transition from enzalutamide resistance to neuroendocrine differentiation (NED).<sup>31</sup> In fact, as revealed in our study and others,<sup>9,10</sup> ADT has a positive impact on the development of NED, which in turn facilitates ADT resistance. Furthermore, the present study indicates that ADT induces the expression of gankyrin in clinical samples and an orthotopic prostate cancer model and that gankyrin promotes progression

and ADT resistance in prostate cancer. In a variety of tumor cells, the oncoprotein gankyrin, as a chaperone of the 26S proteasome, usually relies on its tumor-promoting ability on the degradation of the tumor suppressors p53 and Rb1 via the ubiquitin–proteasome system.<sup>32</sup> Enzalutamide-induced protein degradation, however, is mediated only to a limited extent via the 26S proteasome in prostate cancer cells.<sup>33</sup> Moreover, gankyrin knockdown has a limited influence on proteasome activity in hepatoma carcinoma cells.<sup>19</sup> Therefore, we hypothesized the existence of a proteasome-independent mechanism responsible for gankyrin-mediated ADT resistance in prostate cancer. Consistent with this notion, we found that gankyrin activated the NONO/AR/HMGB1 signaling pathway responsible for the therapy resistance of prostate cancer.

Although most cancer studies have paid close attention to the internal characteristics of tumor cells, the TME, particularly the presence of TAMs, which induce cancer progression, metastasis and acquisition of therapy resistance,<sup>13</sup> should receive adequate attention in investigations of the mechanism underlying ADT resistance. Numerous immune cells, including macrophages, antigen-presenting cells, natural killer cells, T and B lymphocytes, and dendritic cells, are vital components of the TME.<sup>34</sup> However, the composition of the TME varies between cancer types. In ADT-treated prostate cancer, T cells (with a 1.87-fold increase) and macrophages (with a 1.78-fold increase) are the main immune cells that infiltrated the TME.<sup>35</sup> Interestingly, macrophages seemingly act as a bridge between T cells and cancer cells in the prostate cancer TME. In the TRAMP prostate cancer model, an immunocompetent model, CD4<sup>low</sup>HLA-G<sup>+</sup> T cells facilitate the AR-independent proliferation of prostate cancer cells via CD11b<sup>low</sup>F4/80<sup>hi</sup> macrophages,<sup>36</sup> whereas invariant natural killer T cells selectively promote M1 macrophage survival and M2 macrophage death to retard prostate cancer progression.<sup>37</sup> Herein, placing special emphasis on the “bridge cells” TAMs, the present research was performed using a T-cell-deficient but normal macrophage nude mouse model. Our studies and those of others have demonstrated that TAMs release various cytokines and secretory signaling molecules, such as VEGF, HMGB1 and IL-6,<sup>8,9,38</sup> to facilitate prostate cancer therapeutic resistance and progression. Moreover, HMGB1 serves as a primary marker of immunogenic cell death (ICD), which plays a critical role in inducing the antitumor immune response and triggering cancer cell death in prostate cancer.<sup>39</sup> Here, we provide further evidence showing that gankyrin may serve as an upstream regulator of HMGB1 by inducing the recruitment, retention and M2 polarization of macrophages. Furthermore, HMGB1-induced TAM polarization was found to enhance the expression of gankyrin via IL-6-STAT3 signaling. Thus, we successfully identified the network that governs the interaction between gankyrin-mediated ADT resistance and TAMs. Additionally, whether the gankyrin-associated ubiquitin–proteasome system or HMGB1-related ICD could mechanistically be involved in prostate cancer progression or metastasis is worth investigating in further research.

(shGankyrin) were subcutaneously injected into castrated BALB/c nude mice (n = 5/group). Visual examination of isolated tumors from the groups is presented (k). The statistical analysis of tumor volume in the indicated groups after inoculation is presented (l). (m), Schematic illustration showing the potential signaling pathways of gankyrin involved in prostate cancer progression (\*p < .05, \*\*p < .01 and \*\*\*p < .001).

Moreover, to investigate the prognostic value of gankyrin in prostate cancer patients, we combined gankyrin with clinical predictors such as the Gleason score, TNM stage or PSA and found significantly enhanced prognostic accuracy for the BCR and DFS of prostate cancer patients compared to the use of gankyrin or other indicators alone. Therefore, when combined with existing clinical indicators, gankyrin might serve as a reliable predictor of clinical outcomes and therapeutic response in prostate cancer patients, which may be helpful in distinguishing different subgroups of patients to tailor individualized therapeutic options. Our future studies will clarify the prognostic value of gankyrin in prostate cancer patients in multicenter clinical samples and determine whether blocking gankyrin-related pathways can improve the sensitivity of targeted therapy and immunotherapy of prostate cancer using more preclinical models.

## Abbreviations

CRPC: Castration resistant prostate cancer; TAM: tumor-associated macrophage; CHIP: Chromatin immunoprecipitation; ADT: Androgen deprivation therapy; PSA: Prostate Specific Antigen; NONO: non-POU-domain-containing octamer-binding protein HMGB1: High Mobility Group Box 1; TME: Tumor microenvironment; ELISA: Enzyme linked immune sorbent assay; GS: Gleason score; BPH: Benign prostatic hyperplasia; BCR: Biochemical recurrence; DFS: Disease free survival; CM: conditioned medium; ROC: receiver operating characteristics; GEO: Gene Expression Omnibus

## Availability of data and materials

All data generated or analyzed during this study are included in this published article and its supplemental materials.

## Disclosure statement

The authors have declared that no competing interest exists

## Funding

This work was supported by the National Natural Science Foundation of China (No. 82173357, 81773154), Shanghai Natural Science Foundation (No. 20ZR1449600), Pudong New Area Science and technology development fund special fund for people's livelihood Research (medical and health) (PKJ2019-Y19), The Top-level Clinical Discipline Project of Shanghai Pudong (PWYgf2018-03), Construction of clinical peak discipline of Shanghai Pudong New Area Health Committee (PYWgf2021-06), Shanghai Sailing Program (19YF1447000), the Science and Technology Foundation of the Health Commission of Guizhou province (gzwkj2022-102).

## Author contributions

Guang Peng, Chao Wang, Yuquan Jiang, Sishun Gan, and Xu Gao designed and organize the implementation of the project; Chao Wang, Guang Peng, Hongru Wang, Min Qu, Keqin Dong, Yongwei Yu collected and assembled the data. Chao Wang, Guang Peng, Hongru Wang, Min Qu, and Keqin Dong analyzed the data; Guang Peng and Chao Wang wrote the manuscript. The final paper was approved by all of the authors.

## References

- Huggins C, Hodges CV. Studies on Prostatic Cancer. I. The Effect of Castration, of Estrogen and of Androgen Injection on Serum Phosphatases in Metastatic Carcinoma of the Prostate. *J Urol.* 1972;167(2):948–951. doi:10.1016/S0022-5347(02)80307-X.
- Davis ID, Martin AJ, Stockler MR, Begbie S, Chi KN, Chowdhury S, Coskinas X, Frydenberg M, Hague WE, Horvath LG, *et al.* Enzalutamide with Standard First-Line Therapy in Metastatic Prostate Cancer. *NEJM.* 2019;381(2):121–131. doi:10.1056/NEJMoa1903835.
- Chi KN, Agarwal N, Bjartell A, Chung BH, Pereira de Santana Gomes AJ, Given R, Juárez Soto Á, Merseburger AS, Özgüroğlu M, Uemura H, *et al.* Apalutamide for Metastatic, Castration-Sensitive Prostate Cancer. *NEJM.* 2019;381(1):13–24. doi:10.1056/NEJMoa1903307.
- Nuhn P, De Bono JS, Fizazi K, Freedland SJ, Grilli M, Kantoff PW, Sonpavde G, Sternberg CN, Yegnasubramanian S, Antonarakis ES. Update on Systemic Prostate Cancer Therapies: management of Metastatic Castration-resistant Prostate Cancer in the Era of Precision Oncology. *Eur Urol.* 2019;75(1):88–99. doi:10.1016/j.eururo.2018.03.028.
- Arora Vivek K, Schenkein E, Murali R, Subudhi Sumit K, Wongvipat J, Balbas Minna D, Shah N, Cai L, Efstathiou E, Logothetis C, *et al.* Glucocorticoid Receptor Confers Resistance to Antiandrogens by Bypassing Androgen Receptor Blockade. *Cell.* 2013;155(6):1309–1322. doi:10.1016/j.cell.2013.11.012.
- Paschalis A, Sharp A, Welti JC, Neeb A, Raj GV, Luo J, Plymate SR, de Bono JS. Alternative splicing in prostate cancer. *Nat Rev Clin Oncol.* 2018;15(11):663–675. doi:10.1038/s41571-018-0085-0.
- Antonarakis ES, Lu C, Wang H, Lubner B, Nakazawa M, Roeser JC, Chen Y, Mohammad TA, Chen Y, Fedor HL, *et al.* AR-V7 and Resistance to Enzalutamide and Abiraterone in Prostate Cancer. *NEJM.* 2014;371(11):1028–1038. doi:10.1056/NEJMoa1315815.
- Huang H, Wang C, Liu F, Li HZ, Peng G, Gao X, Dong KQ, Wang HR, Kong DP, Qu M, *et al.* Reciprocal Network between Cancer Stem-Like Cells and Macrophages Facilitates the Progression and Androgen Deprivation Therapy Resistance of Prostate Cancer. *Clin Cancer Res.* 2018;24(18):4612–4626. doi:10.1158/1078-0432.CCR-18-0461.
- Wang C, Peng G, Huang H, Liu F, Kong DP, Dong KQ, Dai LH, Zhou Z, Wang KJ, Yang J, *et al.* Blocking the Feedback Loop between Neuroendocrine Differentiation and Macrophages Improves the Therapeutic Effects of Enzalutamide (MDV3100) on Prostate Cancer. *Clin Cancer Res.* 2018;24(3):708–723. doi:10.1158/1078-0432.CCR-17-2446.
- Zhang Y, Zheng D, Zhou T, Song H, Hulsurkar M, Su N, Liu Y, Wang Z, Shao L, Ittmann M, *et al.* Androgen deprivation promotes neuroendocrine differentiation and angiogenesis through CREB-EZH2-TSP1 pathway in prostate cancers. *Nat Commun.* 2018;9(1):5.
- Kato M, Placencio-Hickok VR, Madhav A, Haldar S, Tripathi M, Billet S, Mishra R, Smith B, Rohena-Rivera K, Agarwal P, *et al.* Heterogeneous cancer-associated fibroblast population potentiates neuroendocrine differentiation and castrate resistance in a CD105-dependent manner. *Oncogene.* 2019;38(5):716–730. doi:10.1038/s41388-018-0461-3.
- Sun Y. Tumor microenvironment and cancer therapy resistance. *Cancer Lett.* 2016;380(1):205–215. doi:10.1016/j.canlet.2015.07.044.
- Noy R, Pollard JW. Tumor-associated macrophages: from mechanisms to therapy. *Immunity.* 2014;41(1):49–61. doi:10.1016/j.immuni.2014.06.010.
- Ginhoux F, Schultze JL, Murray PJ, Ochando J, Biswas SK. New insights into the multidimensional concept of macrophage ontogeny, activation and function. *Nat Immunol.* 2016;17(1):34–40. doi:10.1038/ni.3324.
- Escamilla J, Schokrpur S, Liu C, Priceman SJ, Moughon D, Jiang Z, Pouliot F, Magyar C, Sung JL, Xu J, *et al.* CSF1 Receptor Targeting in Prostate Cancer Reverses Macrophage-Mediated Resistance to



- Androgen Blockade Therapy. *Cancer Res.* 2015;75(6):950–962. doi:10.1158/0008-5472.CAN-14-0992.
16. Camacho-Moll ME, Macdonald J, Looijenga LHJ, Rimmer MP, Donat R, Marwick JA, Shukla CJ, Carragher N, Jørgensen A, Mitchell RT. The oncogene Gankyrin is expressed in testicular cancer and contributes to cisplatin sensitivity in embryonal carcinoma cells. *BMC Cancer.* 2019;19(1). doi:10.1186/s12885-019-6340-7.
  17. Chen J, Bai M, Ning C, Xie B, Zhang J, Liao H, Xiong J, Tao X, Yan D, Xi X, *et al.* Gankyrin facilitates follicle-stimulating hormone-driven ovarian cancer cell proliferation through the PI3K/AKT/HIF-1 $\alpha$ /cyclin D1 pathway. *Oncogene.* 2015;35(19):2506–2517. doi:10.1038/ncr.2015.316.
  18. Zhen C, Chen L, Zhao Q, Liang B, Gu YX, Bai Z, Wang K, Xu X, Han Q, Fang D, *et al.* Gankyrin promotes breast cancer cell metastasis by regulating Rac1 activity. *Oncogene.* 2012;32(29):3452–3460. doi:10.1038/ncr.2012.356.
  19. Luo T, Fu J, Xu A, Su B, Ren Y, Li N, Zhu J, Zhao X, Dai R, Cao J, *et al.* PSMD10/gankyrin induces autophagy to promote tumor progression through cytoplasmic interaction with ATG7 and nuclear transactivation of ATG7 expression. *Autophagy.* 2016;12(8):1355–1371. doi:10.1080/15548627.2015.1034405.
  20. Wang C, Li Y, C-m C, X-m Z, Ma J, Huang H, Y-n W, T-y H, Zhang J, X-w P, *et al.* Gankyrin is a novel biomarker for disease progression and prognosis of patients with renal cell carcinoma. *EBioMedicine.* 2019;39:255–264. doi:10.1016/j.ebiom.2018.12.011.
  21. Wang C, Wang Y, Hong T, Cheng B, Gan S, Chen L, Zhang J, Zuo L, Li J, Cui X. Blocking the autocrine regulatory loop of Gankyrin/STAT3/CCL24/CCR3 impairs the progression and pazopanib resistance of clear cell renal cell carcinoma. *Cell Death Dis.* 2020;11(2):117. doi:10.1038/s41419-020-2306-6.
  22. Sakurai T, Yada N, Hagiwara S, Arizumi T, Minaga K, Kamata K, Takenaka M, Minami Y, Watanabe T, Nishida N, *et al.* Gankyrin induces STAT3 activation in tumor microenvironment and sorafenib resistance in hepatocellular carcinoma. *Cancer Sci.* 2017;108(10):1996–2003. doi:10.1111/cas.13341.
  23. Riahi MM, Sistani NS, Zamani P, Abnous K, Jamialahmadi K. Correlation of Gankyrin oncoprotein overexpression with histopathological grade in prostate cancer. *Neoplasma.* 2017;64(5):732–737. doi:10.4149/neo\_2017\_511.
  24. Kim TD, Oh S, Lightfoot SA, Shin S, Wren JD, Janknecht R. Upregulation of PSMD10 caused by the JMJD2A histone demethylase. *Int J Clin Exp Med.* 2016;9:10123–10134.
  25. Vanaja DK, Cheville JC, Iturria SJ, Young CYF. Transcriptional silencing of zinc finger protein 185 identified by expression profiling is associated with prostate cancer progression. *Cancer Res.* 2003;63:3877–3882.
  26. Takayama KI, Suzuki T, Fujimura T, Yamada Y, Takahashi S, Homma Y, Suzuki Y, Inoue S. Dysregulation of spliceosome gene expression in advanced prostate cancer by RNA-binding protein PSF. *Proc Natl Acad Sci U S A.* 2017;114(39):10461–10466. doi:10.1073/pnas.1706076114.
  27. Wang J, Zou JX, Xue X, Cai D, Zhang Y, Duan Z, Xiang Q, Yang JC, Louie MC, Borowsky AD, *et al.* ROR-gamma drives androgen receptor expression and represents a therapeutic target in castration-resistant prostate cancer. *Nat Med.* 2016;22(5):488–496. doi:10.1038/nm.4070.
  28. Bieniasz-Krzywiec P, Martin-Perez R, Ehling M, Garcia-Caballero M, Pinioti S, Pretto S, Kroes R, Aldeni C, Di Matteo M, Prenen H, *et al.* Podoplanin-Expressing Macrophages Promote Lymphangiogenesis and Lymphoinvasion in Breast Cancer. *Cell Metab.* 2019;30(5):917–936 e910. doi:10.1016/j.cmet.2019.07.015.
  29. Sahraei M, Chaube B, Liu Y, Sun J, Kaplan A, Price NL, Ding W, Oyaghire S, Garcia-Milian R, Mehta S, *et al.* Suppressing miR-21 activity in tumor-associated macrophages promotes an antitumor immune response. *J Clin Invest.* 2019;129(12):5518–5536. doi:10.1172/JCI127125.
  30. Chen K, Cao Q, Song Z, Ruan H, Wang C, Yang X, Bao L, Wang K, Cheng G, Xu T, *et al.* Targeting the KIF4A/AR axis to reverse endocrine therapy resistance in castration-resistant prostate cancer. *Clin Cancer Res.* 2019.
  31. Liu B, Li L, Yang G, Geng C, Luo Y, Wu W, Manyam GC, Korentzelos D, Park S, Tang Z, *et al.* PARP Inhibition Suppresses GR-MYCN-CDK5-RB1-E2F1 Signaling and Neuroendocrine Differentiation in Castration-Resistant Prostate Cancer. *Clin Cancer Res.* 2019;25(22):6839–6851. doi:10.1158/1078-0432.CCR-19-0317.
  32. Higashitsuji H, Higashitsuji H, Itoh K, Sakurai T, Nagao T, Sumitomo Y, Masuda T, Dawson S, Shimada Y, Mayer RJ, *et al.* The oncoprotein gankyrin binds to MDM2/HDM2, enhancing ubiquitylation and degradation of p53. *Cancer Cell.* 2005;8(1):75–87.
  33. Erb HHH, Oster MA, Gelbrich N, Cammann C, Thomas C, Mustea A, Stope MB. Enzalutamide-induced Proteolytic Degradation of the Androgen Receptor in Prostate Cancer Cells Is Mediated Only to a Limited Extent by the Proteasome System. *Anticancer Res.* 2021;41(7):3271–3279. doi:10.21873/anticancer.15113.
  34. Anderson NM, Simon MC. The tumor microenvironment. *Curr Biol.* 2020;30(16):R921–R925. doi:10.1016/j.cub.2020.06.081.
  35. Gannon PO, Poisson AO, Delvoe N, Lapointe R, Mes-Masson AM, Saad F. Characterization of the intra-prostatic immune cell infiltration in androgen-deprived prostate cancer patients. *J Immunol Methods.* 2009;348(1–2):9–17. doi:10.1016/j.jim.2009.06.004.
  36. Wang C, Chen J, Zhang Q, Li W, Zhang S, Xu Y, Wang F, Zhang B, Zhang Y, Gao WQ. Elimination of CD4(low)HLA-G(+) T cells overcomes castration-resistance in prostate cancer therapy. *Cell Res.* 2018;28(11):1103–1117. doi:10.1038/s41422-018-0089-4.
  37. Cortesi F, Delfanti G, Grilli A, Calcinotto A, Gorini F, Pucci F, Luciano R, Grioni M, Recchia A, Benigni F, *et al.* Bimodal CD40/Fas-Dependent Crosstalk between iNKT Cells and Tumor-Associated Macrophages Impairs Prostate Cancer Progression. *Cell Rep.* 2018;22(11):3006–3020. doi:10.1016/j.celrep.2018.02.058.
  38. Chen PC, Cheng HC, Wang J, Wang SW, Tai HC, Lin CW, Tang CH. Prostate cancer-derived CCN3 induces M2 macrophage infiltration and contributes to angiogenesis in prostate cancer microenvironment. *Oncotarget.* 2014;5(6):1595–1608. doi:10.18632/oncotarget.1570.
  39. Li C, Zhang Y, Yan S, Zhang G, Wei W, Qi Z, Li B. Alternol triggers immunogenic cell death via reactive oxygen species generation. *Oncoimmunology.* 2021;10(1):1952539. doi:10.1080/2162402X.2021.1952539.